Available online at www.sciencedirect.com

SciVerse ScienceDirect

Procedia CIRP 8 (2013) 81 – 87

www.elsevier.com/locate/procedia

14th CIRP Conference on Modeling of Machining Operations (CIRP CMMO)

Machining of Difficult-to-Cut-Alloys Using Rotary Turning Tools

Utku Olgun and Erhan Budak*

[a]*Manufacturing Research Laboratory, Sabancı University, İstanbul, Turkey*

* Corresponding author. Tel.: +90 216 483 9519; fax: +90 216 4839550.*E-mail address*: ebudak@sabanciuniv.edu.

Abstract

The importance and use of high temperature metals, such as titanium and nickel alloys, in aerospace industries have been continuously increasing due to their high strength-to-weight properties. These superior mechanical properties, however, reduce the machinability of these alloys. Rotary turning tools offer remedy to these problems. Rotary motion of the insert provides cool-down time outside of the cut resulting reduced cutting temperatures with longer tool life and higher productivity. In this article, rotary and stationary turning tools are compared in terms of tool life, cutting forces, surface and dimensional quality.

Selection and peer-review under responsibility of The International Scientific Committee of the "14th CIRP Conference on Modeling of Machining Operations" in the person of the Conference Chair Prof. Luca Settineri

Keywords:Rotary Turning, Difficult-to-cut alloys, Machinability

1 Introduction

Heat-resistant materials have received interest in aerospace and defense industries due to their superior strength-to-weight ratio [1,2]. Owing to their low thermal conductivity, the generated heat results in higher cutting temperatures, reduce machinability and thus make them difficult to machine. In order to increase the machinability, different tooling materials have been tried. Carbides are usually used at low speeds to have economic tool life at the cost of increased machining time. Ceramics are not preferred due to their low shock capacity. CBN, PCBN, and PCD tools can be solution for machining these alloys; however, they are expensive [3].

Rotary turning can be a remedy to increase the machinability of these alloys. Round insert rotates continuously about its own axis during cutting and tool rotation distributes the cutting energy to the whole circular edge. There are two types of rotary tools; self-propelled (SPRT) and actively driven (ADRT) as shown in Figure 1. In SPRT, rotary motion of the insert is achieved by its interaction with the workpiece, however in ADRT, an external motor is used to control the insert rotational speed.

Shaw [4] observed a similarity between the rotary turning process and the classical oblique cutting. Venuvinod [5] and Armarego [6] modeled the kinematics and mechanics of rotary cutting processes. They claimed that rotary cutting process is kinematically and mechanically equivalent to classical cutting processes, but the friction conditions prevent perfect equivalency. The temperature change of rotary cutting tools during the process has been modeled in several works to understand the thermal behavior [7,8]. Furthermore, rotary tools exhibit superior wear resistance, lower cutting temperatures and forces owing to reduced amount of work done and friction on the rake face [9,10]. The effects of rotary tool's speed, inclination angle, cooling conditions on the cutting temperature with ADRT tools were also investigated [11,12].

In this study, an experimental approach is used to determine the effects of cutting parameters on the rotary process. In addition, the cutting performance of rotary tools is evaluated for several materials, cooling systems and cutting parameters as well as tool rotational speed and inclination.

Selection and peer-review under responsibility of The International Scientific Committee of the "14th CIRP Conference on Modeling of Machining Operations" in the person of the Conference Chair Prof. Luca Settineri

doi:10.1016/j.procir.2013.06.069

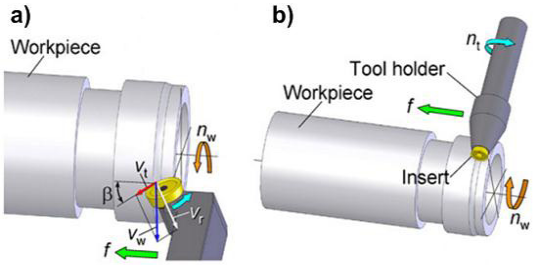

Figure 1:Types of rotary turning tools, a) SPRT and b) ADRT [11].

2 Process Mechanics

It is significant to model rotary turning process to gain deeper understanding of the process in relation to classical cutting processes. Introducing the motion of insert to the system, as in Figure 2, makes the process more complicated. The presented analysis depends on tube-end cutting for simplification. There are some assumptions to simplify the analysis [13];

- Cutting edge curvature is ignored since the radius of insert is higher than the tube thickness.
- The direction between the friction force vector and the relative chip flow vector, and the direction between the shear force vector and the shear velocity vector are assumed to be collinear.

Rotary turning process incorporates the motion of the round insert in addition to the workpiece velocity bringing effective cutting velocity, at an angle to normal plane of the cutting edge as in the case of oblique cutting process (Figure 2). Moreover, rotary tool velocity affects the chip flow angle such that absolute chip flow velocity direction and magnitude change with different friction conditions.

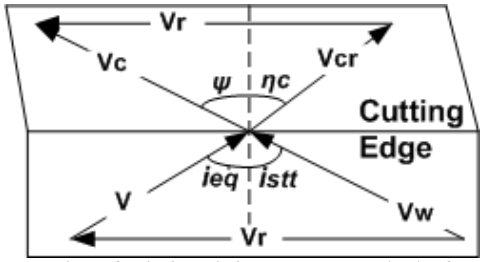

Figure 2: View of velocity relations on rotary tool rake face and workpiece cutting face.

According to Figure 2, velocity relations that are purely kinematic can be expressed as;

$$\overrightarrow{V_w} = \vec{V} + \overrightarrow{V_r} \quad (1)$$

$$\overrightarrow{V_c} = \overrightarrow{V_{cr}} + \overrightarrow{V_r} \quad (2)$$

Cutting velocity, V_w, is the sum of effective cutting velocity, V and rotary tool velocity, V_r. Similarly, absolute chip velocity,V_c, is the sum of the relative chip velocity, V_{cr} and rotary tool velocity. Using these relations, the equivalent inclination angle, $i_{eq}$is expressed as [6];

$$V * \cos(i_{eq}) = V_w * \cos(i_{stt}) \quad (3)$$

$$\tan(i_{eq}) = \frac{V_r + V_w * \sin(i_{stt})}{V_w * \cos(i_{stt})} \quad (4)$$

where i_{eq} is the angle between effective cutting velocity and normal plane of the cutting edge, i_{stt} is the angle between cutting velocity and normal plane of the cutting edge (Figure 2). In order to provide the equivalency with classical cutting operations, the cutting mechanism should be studied in the plane of V-V_{cr} due to the rotary motion of the insert.

Effective rake angle as in classical oblique cutting is an advantage and defined as [4];

$$\sin(\alpha_e) = sin(\eta_c) * sin(i_{eq}) + cos(\eta_c) * cos(i_{eq}) * sin(\alpha_n) \quad (5)$$

where $\alpha_e$is effective rake angle and$\eta_c$is relative chip flow angle.

The effective rake angle variations with rotary tool velocity for various cutting speed are shown in Figure 3 using equation (5).

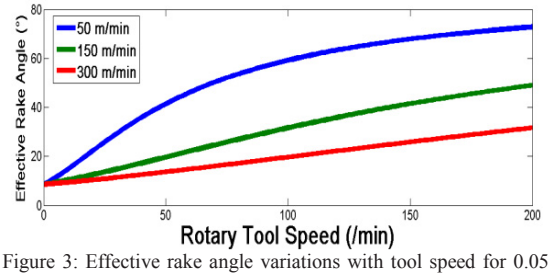

Figure 3: Effective rake angle variations with tool speed for 0.05 mm/rev feed, 2.05 mm depth of cut, 150m/min cutting speed.

Results show that effective rake angle increases in a range of rotary tool speed. Low cutting speeds are favorable as they result in higher effective rake angles during the process.

As shown in Figure 4, the component forces are defined as in conventional oblique cutting process. Static and equivalent inclination angles are incorporated in the equations in order to provide equivalency in chip widths and material removal rates between rotary and conventional processes.

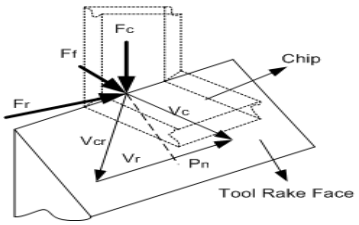

Figure 4: Component forces in rotary cutting.

Tangential, radial and feed cutting forces are expressed, respectively [6];

$$F_T = \frac{\tau * t * B * \cos(i_{eq})}{\sin(\Phi_n) * \cos(i_{stt})} * \frac{[\cos(\beta_n - \alpha_n) + \sin(\beta_n) * \tan(\eta_c) * \tan(i_{eq})]}{\sqrt{\cos^2(\Phi_n + \beta_n - \alpha_n) + \tan^2(\eta_c) * \sin^2(\beta_n)}} \quad (6)$$

$$F_R = \frac{\tau * t * B * \cos(i_{eq})}{\sin(\Phi_n) * \cos(i_{stt})} * \frac{[\cos(\beta_n - \alpha_n) * \tan(i_{eq}) - \tan(\eta_c) * \sin(\beta_n)]}{\sqrt{\cos^2(\Phi_n + \beta_n - \alpha_n) + \tan^2(\eta_c) * \sin^2(\beta_n)}} \quad (7)$$

$$F_F = \frac{\tau * t * B}{\sin(\Phi_n) * \cos(i_{stt})} * \frac{\sin(\beta_n - \alpha_n)}{\sqrt{\cos^2(\Phi_n + \beta_n - \alpha_n) + \tan^2(\eta_c) * \sin^2(\beta_n)}} \quad (8)$$

where B is the chip width. Cutting parameters from orthogonal cutting tests are utilized to simulate rotary turning process. Normal friction (β_n), shear stress τ, normal shear angle (Φ_n), chip thickness ratio values are taken from orthogonal database to predict forces. The turning process is simulated by dividing the contact zone between the circular insert and the workpiece into elements. The forces are calculated for each element and the total force is obtained by summing them up. The contact length is calculated by using Dawson and Kurfess [14] contact length model:

$$L_c = R * \left[\cos^{-1}\left(\frac{R - d_{eff}}{R}\right) + \tan^{-1}\left(\frac{f}{2 * R}\right)\right] \quad (9)$$

where R is radius of round insert, f is feed, d_{eff} is effective depth. Effective depth depends on tool inclination and is given by;

$$d_{eff} = \frac{d}{\cos(i_{stt})} \quad (10)$$

3 Experimental Procedure

3.1 Self-Propelled Rotary Turning Tool Cutting Tests

Self-propelled rotary tool (SPRT) tests were carried out on Mori Seiki NL1500 turning center. The SPRT tool is attached to the turret as shown in Figure 5. The testing workpiece materials are 1050 steel, Waspaloy and Ti6Al4V.

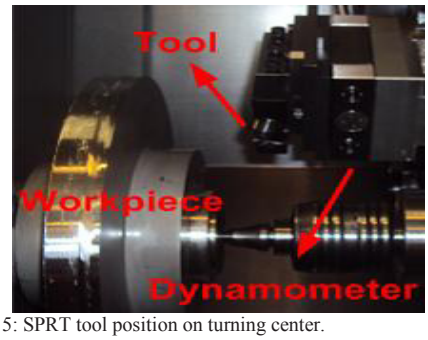

Figure 5: SPRT tool position on turning center.

Dry, flood coolant and MQL cooling conditions are applied for all test materials. The holder used for SPRT is patented design of Rotary Technologies Corporation [15]. The carbide insert used has a coating of Alcrona [15], and has 27 mm diameter and 0° rake and clearance angles. Insert cartridge and tool holder together provide -15° of rake and 5° of effective clearance to cutting edge. In order to compare with the performance of the SPRT, stationary tool tests were also done. The carbide insert used in stationary tool cutting tests has CVD coating. It has 13 mm diameter with -6° rake, -6° oblique and 6° clearance angles.

Cutting forces are measured using three-dimensional Kistler dynamometer whereas Nanofocus μsurf surface metrology system is used for surface roughness and flank wear measurements. A CMM is used to evaluate the roundness of machined workpieces. 400 m/min cutting speed, 0.2 mm/rev feed and 1 mm depth of cut are the cutting parameters for 1050 steel. 45 m/min cutting speed, 0.1 mm/rev feed and 0.2 mm depth of cut values are used in Waspaloy and Ti6Al4V tests. Conditions for cutting tests can be seen in Table 1.

Table 1: Experiment Conditions for cutting tests.

Test No	Workpiece	Tooling	Cooling
1	AISI 1050	Stationary	Dry
2	AISI 1050	SPRT	Dry
3	AISI 1050	SPRT	Coolant
4	Waspaloy	Stationary	Dry
5	Waspaloy	SPRT	Dry
6	Waspaloy	SPRT	Coolant

7	Waspaloy	SPRT	MQL
8	Ti6Al4V	Stationary	Dry
9	Ti6Al4V	Stationary	Coolant
10	Ti6Al4V	SPRT	Dry
11	Ti6Al4V	SPRT	Coolant
12	Ti6Al4V	SPRT	MQL

3.1.1 Tool Wear

Due to spinning motion of SPRT tool, shorter tool-workpiece engagement time is obtained. All cutting energy is spread to the overall circular cutting edge since the whole perimeter of insert is involved in operation. Insert motion reduces amount of work done and friction on the tool rake [9] resulting easy shearing and lower cutting temperatures. The performance comparisons of SPRT and stationary tool for 1050, Waspaloy and Ti6Al4V alloy for dry, flood coolant and MQL conditions are presented in Figure 6, Figure 7, Figure 8, respectively. It is obvious that SPRT tool exhibits superior wear resistance compared to stationary tool.

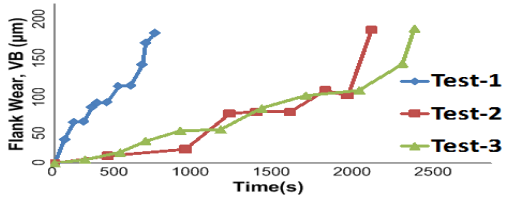

Figure 6: Tool wear variation with time for 1050 steel for different testing conditions

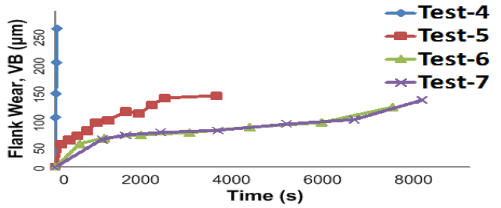

Figure 7: Tool wear variation with time for Waspaloy for different testing conditions.

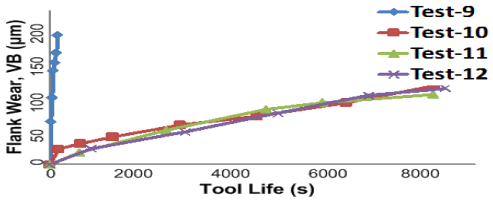

Figure 8: Tool wear variation with time for Ti6Al4V for different testing conditions.

Even though stationary insert can be used 18 times by shifting its edge, SPRT tool rotation still improves the total life of the insert up to5folds and 4.3folds, in Waspaloy and Ti6Al4V tests, respectively, under dry cutting conditions. In Waspaloy tests, coolant and MQL improve tool life 100% compared to dry cutting condition. In 1050 steel, flood coolant increases tool life 14% in comparison to dry cutting. However, in Ti6Al4V tests, all cooling conditions exhibit the same tool wear trend.

Uniformly distributed flank wear is the main failure mechanism in SPRT operation and crater wear is not observed on the tool rake. In Waspaloy and Ti6Al4V tests, the stationary tool is exposed to high cutting temperatures and high friction conditions causing high rate of flank wear, burning on cutting edge and extreme crater formation on rake face as shown in Figure 9.

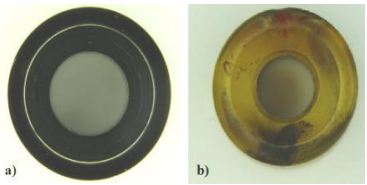

Figure 9: Figure Rake faces of worn tools a) SPRT b) Stationary tool.

3.1.2 Cutting Forces

The measured cutting forces in tangential, radial and feed directions for different tooling systems for Ti6Al4V cutting tests are shown in Figure 10.

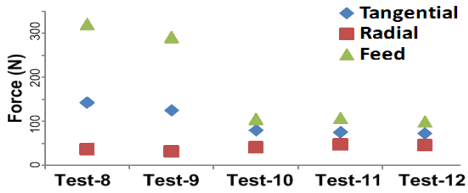

Figure 10: Measured tangential cutting forces for stationary and SPRT tool.

Component forces except radial forces are reduced when machining with SPRT tool compared to the stationary tool in machining of Ti6Al4V. In machining of Ti6Al4V, the tangential and feed forces with SPRT are 42% and 64% lower than those generated in stationary tool, respectively. However, higher the radial forces are obtained mainly due to increased effective oblique angle. The effect of the coolant is more distinct in stationary tool cutting forces. The tangential cutting forces decrease 12% compared to dry conditions during machining of Ti6Al4V whereas they are almost the same for SPRT.

3.1.3 Surface Roughness and Circularity

The surface generated with SPRT has a cutting trace at an angle to the feed direction due to the spinning action that can be seen in Figure 11 for Test-1 and Test-2.

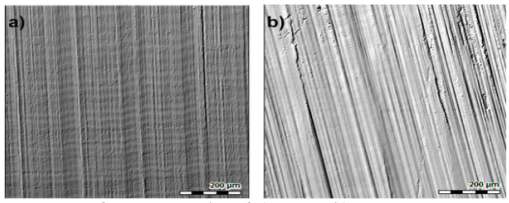

Figure 11: Surface topography of a) Test-1 b) Test-2.

The roughness and roundness measurements are summarized in Table 2. The roughness in circumferential direction in SPRT tool is better than that of the stationary tool. However, the roughness in the feed direction is increased significantly in SPRT. This could be caused by the lower rigidity and higher eccentricity of the rotary tooling which needs further investigation. The difference in the circularities for two processes is not remarkable but the circularity with the stationary tool is slightly better compared to SPRT.

Table 2: Surface roughness and circularity measurement results for Test-1 and Test-2.

	Stationary	SPRT
Roughness in FeedDir.	0.30µm	0.65µm
Roughness in Cir.Dir.	1.16µm	0.77µm
Circularity	2-3 µm	4-6 µm

3.2 Actively Driven Rotary Turning Tool Cutting Tests

Mori Seiki NTX2000 mill-turn machining center is used for testing of ADRT. This machine includes 9 axes with two chucks, a milling spindle and a turning turret. In order to perform cutting tests, milling spindle whose head moves along the X-, Y- and Z-axes and rotates around the B- axis is utilized to attach a rotary tool holder. The rotary tool speed and rotary tool inclination angle can be controlled by this milling spindle. The test workpiece materials are 1050 steel and Waspaloy. The experimental set-up can be seen in Figure 12.

The tests were conducted under dry, flood coolant and MQL conditions with various cutting parameters. The cutting tool used for ADRT is a carbide insert with multi-layer CVD coating of MT-Ti(C,N)+Al_2O_3+TiN . It has 25 mm diameter with a chip breaker and 7° clearance angle. Tool flank wear and surface roughness measurements are performed with Nanofocus µsurf surface metrology system. 400 m/min cutting speed, 0.2 mm/rev feed and 1 mm depth of cut are the cutting parameters for 1050 steel. 45 m/min cutting speed, 0.1 mm/rev feed and 0.2 mm depth of cut values are used for Waspaloy tests.

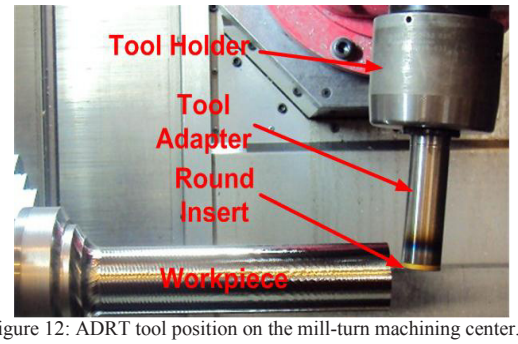

Figure 12: ADRT tool position on the mill-turn machining center.

The cutting conditions are listed in Table 3.

Table 3: Experimental conditions for ADRT tool cutting tests.

Test No	Workpiece	Tool Speed	Tool Inc.	Cooling
13	AISI 1050	50	0	Dry
14	AISI 1050	250	0	Dry
15	AISI 1050	400	0	Dry
16	AISI 1050	50	5	Dry
17	AISI 1050	250	5	Dry
18	AISI 1050	400	5	Dry
19	AISI 1050	50	0	Coolant
20	AISI 1050	250	0	Coolant
21	AISI 1050	400	0	Coolant
22	AISI 1050	50	5	Coolant
23	AISI 1050	250	5	Coolant
24	AISI 1050	400	5	Coolant
25	AISI 1050	50	0	MQL
26	AISI 1050	250	0	MQL
27	AISI 1050	50	5	MQL
28	AISI 1050	250	5	MQL
29	Waspaloy	0	0	Coolant
30	Waspaloy	10	0	Coolant
31	Waspaloy	20	0	Coolant
32	Waspaloy	45	0	Coolant
33	Waspaloy	10	5	Coolant
34	Waspaloy	20	5	Coolant
35	Waspaloy	10	15	Coolant

3.2.1 Tool Wear

Cutting test results indicate that increasing rotary tool speed after a certain range causes higher tool wear rate. Figure 13 shows the variation of the tool life with rotary tool speed for Waspaloy. At very low and high tool speeds, the tool life is the worst, since at lower speeds the contact time between the tool and the workpiece increases whereas at higher speeds, the required time for the tool to cool down is inadequate resulting in heat accumulation at the tool tip.

On the other hand, increasing the rotary tool inclination angle improves the tool life. Figure 14 exhibits the effect of the inclination on the tool life for Waspaloy. Increasing inclination from 0° to 5° increases tool life 44%, while a rise from 5° to 15° causes an increase up to 49% in tool life.

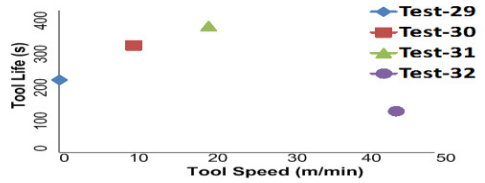

Figure 13: Tool life variation with rotary tool speed for Waspaloy cutting test.

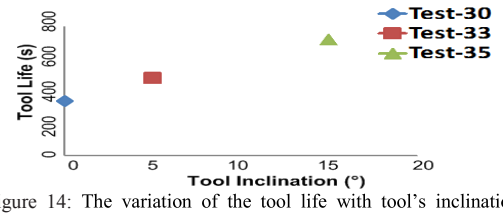

Figure 14: The variation of the tool life with tool's inclination angle for Waspaloy.

The effect of cooling conditions on the tool life for 5° inclination angle, 50 m/min tool speed for 1050 steel is shown in Figure 15.

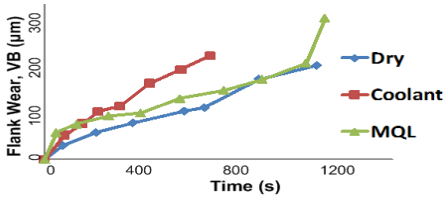

Figure 15: Tool wear progression for AISI 1050 for various cooling conditions.

Dry cutting provides the best tool life results compared to cutting with flood coolant and MQL. Coolant reduces cutting temperature, but it also results in thermal fatigue on the cutting edge lowering the tool life compared to dry cutting.
Tool wear comparisons for SPRT and ADRT are shown in Figure 16.

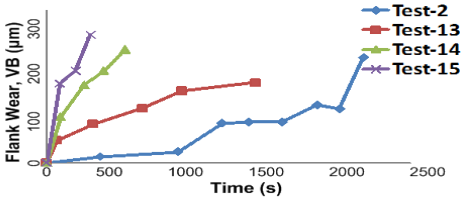

Figure 16: Tool wear comparisons for SPRT and ADRT tests.

Contrary to the expectation, SPRT tool provides the best tool life. Different insert types and coatings are the main reason behind this result. Figure 17 exhibits the variation of the tool life with the tool speed. There is an optimum tool speed range in which minimum tool wear rate and maximum tool life are achieved.

3.2.2 Surface Roughness and Circularity

Figure 18 exhibits the surface topography of Test-27, Test-22 and Test-19, respectively. At 5° tool inclination, as in SPRT process, cutting traces on the surface can be seen at an angle to the feed direction due to tool spinning. Table 4 presents the surface roughness and roundness measurement results.

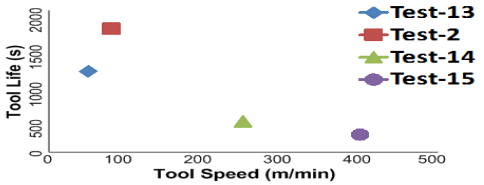

Figure 17: Tool life variation with tool speed for different tools.

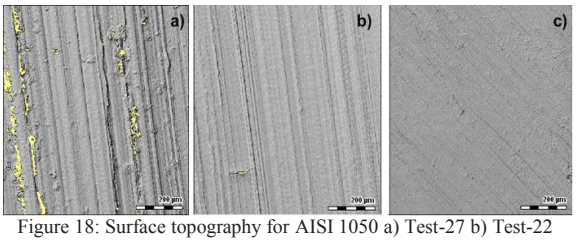

Figure 18: Surface topography for AISI 1050 a) Test-27 b) Test-22 c) Test-19.

Table 4: Surface Roughness and Circularity for Test-27, Test-22 and Test-19.

	Test-27	Test-22	Test-19
Roughness in FeedDir	2.66μm	1.22μm	0.92μm
Roughness in Cir. Dir.	1.33μm	1.39μm	1.44μm
Circularity	35-43 μm	69-85 μm	29-30m

Increasing the tool inclination does not effect roughness in circumferential direction too much, yet the surface quality in feed direction becomes poor. MQL provides the worst roughness in the feed direction. In addition, circularity results show that further investigations are required to improve the rotary process.

4 Conclusions

The following points are concluded:

- Superior tool wear resistance and extended tool life are achieved in rotary turning process due to reduced cutting speed and self-cooling of tool.
- Increasing tool inclination angle results in longer tool life.
- Cutting with flood coolant and MQL have positive effects on the tool life for SPRT due to easy removal of heat from cutting region. On the other

hand, dry cutting condition gives the best tool life results in ADRT processes.

- Cutting forces for SPRT were found to be lower than those of stationary tool.
- SPRT shows better surface quality in the circumferential direction while deteriorated surface is obtained in feed direction compared to the stationary tool.
- Use of flood coolant and decreasing tool inclination improves surface roughness in feed direction.
- SPRT process yielded better tool life and machined part quality compared to ADRT process. However, this is mainly due to the special insert used in SPRT tests.

Acknowledgements

The support from Tubitak (Project 110M522) and Pratt and Whitney Canada for this research is appreciated by the authors.

5 References

[1] Ezugwu, E.O., Wang, Z.M., 1997, Titanium Alloys and Their Machinability - A Review, Journal of Materials Processing Technology, 68, 262-274.
[2] Nabhani, F., 2001, Machining of Aerospace Titanium Alloys, Robotics and Computer Integrated Manufacturing, 17, 99-106.
[3] Rahman, M., Seah, W.K.H., Teo, T.T., 1997, The Machinability of Inconel 718, Journal of Materials Processing, 63, 199-204.
[4] Shaw, M.C., Smith, P.A., Cook, N.H., The Rotary Cutting Tool, Transaction of ASME, 74, 1065-1076.
[5] Venuvinod, P.K., Lau, W.S., Reddy, P.N., 1981, Some Investigations into Machining with Driven Rotary Tools, Journal of Engineering for Industry, 103, 469-477.
[6] Armarego, E.J.A., Karri, V., Smith, A.J.R., 1994, Fundamental Studies of Driven and Self-Propelled Rotary Tool Cutting Processes-1: Theoretical Investigation, International Journal of Machine Tool and Manufacture, 34/6, 785-801.
[7] Chen, P., 1992, Cutting Temperatures and Forces in Machining of High-Performance Materials with Self-Propelled Rotary Tool, The Japan Society of Mechanical Engineers, 35/1, 180-185.
[8] Dessoly, V., Melkote, S.N., Lescalier, C., 2004, Modeling and Verification of Cutting Tool Temperatures in Rotary Tool Turning of Hardened Steel, International Journal of Machine Tools and Manufacture, 44, 1463-1470.
[9] Ezugwu, E.O., Olajire, K.A., Wang, Z.M., 2002, Wear Evaluation of a Self-Propelled Rotary Tool When Machining Titanium Alloy IMI 318, Proceedings of the Institution of Mechanical Engineers, Part b: Journal of Engineering Manufacture, 216, 891-897.
[10] Kishawy, H.A. Becze, C.E., McIntosh, D.G., 2004, Tool Performance and Attainable Surface Quality During the Machining of Aerospace Alloys using Self-Propelled Rotary Tools, Journal of Processing Technology, 152, 266-271.
[11] Hosokawa, A., Ueda, T., Onishi, R., Tanaka, R., Furumoto, T., 2010, Turning of Difficult to Machine Materials with Actively Driven Rotary Tool, CIRP Annals - Manufacturing Technology, 59, 89-92.
[12] Sasahara, H., Satake, K., Nakajima, H., Yamamoto, H., Muraki, T., Tsutsumi, M., 2008, High-Speed Rotary Cutting of Difficult to Cut Materials on Multi Tasking Lathe, International Journal of Machine Tools and Manufacture, 48, 841-850.
[13] Li, L., Kishawy, H.A., 2006, A Model for Cutting Forces Generated During Machining with Self-Propelled Rotary Tools, International Journal of Machine Tools and Manufacture, 46, 1388-1394.
[14] Dawson, T.G., Kurfess, T.R., 2006, Modeling the Progression of Flank Wear on Uncoated and Ceramic-Coated Polycrystalline CBN Tools in Hard Turning, Transactions of the ASME, 128, 104-109.
[15] Rotary Technologies Corporation, Rotary Turning Tool, http://www.rotarytech.com/categ- ory_listing.php?id=8